Phosphorylation Status of the Parvovirus Minute Virus of Mice Particle: Mapping and Biological Relevance of the Major Phosphorylation Sites

BEATRIZ MAROTO, JUAN C. RAMÍREZ,† AND JOSÉ M. ALMENDRAL*

Centro de Biología Molecular "Severo Ochoa" (Consejo Superior de Investigaciones Científicas—Universidad Autónoma de Madrid), 28049 Cantoblanco, Madrid, Spain

The core of the VP-1 and VP-2 proteins forming the T=1 icosahedral capsid of the prototype strain of the parvovirus minute virus of mice (MVMp) share amino acids sequence and a common three-dimensional structure; however, the roles of these polypeptides in the virus infection cycle differ. To gain insights into this paradox, the nature, distribution, and biological significance of MVMp particle phosphorylation was investigated. The VP-1 and VP-2 proteins isolated from purified empty capsids and from virions containing DNA harbored phosphoserine and phosphothreonine amino acids, which in two-dimensional tryptic analysis resulted in complex patterns reproducibly composed by more than 15 unevenly phosphorylated peptides. Whereas secondary protease digestions and comigration of most weak peptides in the fingerprints revealed common phosphorylation sites in the VP-1 and VP-2 subunits assembled in capsids, the major tryptic phosphopeptides were remarkably characteristic of either polypeptide. The VP-2-specific peptide named B, containing the bulk of the ^{32}P label of the MVMp particle in the form of phosphoserine, was mapped to the structurally unordered N-terminal domain of this polypeptide. Mutations in any or all four serine residues present in peptide B showed that the VP-2 N-terminal domain is phosphorylated at multiple sites, even though none of them was essential for capsid assembly or virus formation. Chromatographic analysis of purified wild-type (wt) and mutant peptide B digested with a panel of specific proteases allowed us to identify the VP-2 residues Ser-2, Ser-6, and Ser-10 as the main phosphate acceptors for MVMp capsid during the natural viral infection. Phosphorylation at VP-2 N-terminal serines was not necessary for the externalization of this domain outside of the capsid shell in particles containing DNA. However, the plaque-forming capacity and plaque size of VP-2 N-terminal phosphorylation mutants were severely reduced, with the evolutionarily conserved Ser-2 determining most of the phenotypic effect. In addition, the phosphorylated amino acids were not required for infection initiation or for nuclear translocation of the expressed structural proteins, and thus a role at a late stage of MVMp life cycle is proposed. This study illustrates the complexity of posttranslational modification of icosahedral viral capsids and underscores phosphorylation as a versatile mechanism to modulate the biological functions of their protein subunits.

The functions of viral capsids include making contact with cellular receptors on the target cells of the host, intracellular trafficking of the nucleic acid inward to the replication site and outward to the cellular surface, and preservation of vital functions in the environment. Large viruses may code for polypeptides with specific functions for each of these steps, but small viruses must use determinants of a few amino acids to accomplish these life cycle needs. The 20-nm-diameter nonenveloped capsid of the *Parvoviridae* family (60) offers a well-defined model for fine mapping and structural understanding of such a diversity of functions in an icosahedral virus. The structure of parvovirus capsid has been resolved to atomic resolution for the canine parvovirus (CPV) (69), the feline panleukopenia virus (1), strain i of minute virus of mice (MVMi) (3), and an insect parvovirus (*Galleria mellonella* densovirus) (61) and to lower resolution for the human B19 parvovirus (2) and the Aleutian mink disease parvovirus (43). The parvovirus capsid is formed from 60 protein subunits (15, 59) assembled with a T=1 icosahedral symmetry (14, 35). Each subunit fold results in a core composed of an eight-stranded antiparallel β-barrel motif (52) and four large loops forming the features of the capsid surface, like a cylindrical channel at each fivefold icosahedral axis surrounded by a canyon-like depression, a dimple-like depression at each twofold axis, and (except for B19) a spike-like protrusion along each of the threefold axes. Some major functions have been mapped in the parvovirus capsid, such as the immunogenicity of the spike (9, 63), determinants of tropism at the intracellular level at the top and shoulder of the spike for CPV and MVM (5, 8, 15, 27, 49), domains for primary receptor binding in the depression at the threefold axis of B19 (17), and nuclear transport of capsid protein oligomers at a β-strand of MVM (41).

Our understanding of structure-function relationships in viral particles is complicated by the possibility that relevant determinants of capsid functions may not been resolved in the X-ray structure determination averaging procedure (53) if they are displaced in mobile loops of the capsid surface (30), conform transiently, or do so in a low proportion of the capsid subunits. The posttranslational incorporation of phosphate radicals into structural proteins may result in this type of loose determinants in viral capsids. Phosphates play important roles in many viral systems (reviewed in reference 38), and the phosphorylation of structural components can regulate multi-

* Corresponding author. Mailing address: Centro de Biología Molecular "Severo Ochoa" (CSIC-UAM), Universidad Autónoma de Madrid, 28049 Cantoblanco, Madrid, Spain. Phone: 34-91-3978048. Fax: 34-91-3978087. E-mail: JMAlmendral@cbm.uam.es.

† Present address: Centro Nacional de Biotecnología (CSIC), 28049 Cantoblanco, Madrid, Spain.

ple steps of viral multiplication (46, 75), such as maturation (28, 34), nuclear transport (23, 40), encapsidation (32), or stimulation of cellular growth (6). Icosahedral viruses like adenovirus (70) and papillomavirus (22, 58) harbor phosphorylated structural proteins, although the characteristics and roles of these phosphorylations have not been explored in depth. More information is available for polyomavirus (11, 26, 39), in which some phosphorylation sites have been mapped that play a function in viral assembly (4, 25).

The parvovirus MVM is an interesting model system for determining the functional roles of posttranslational modification of proteins in icosahedral viruses, given our previous report of phosphorylated VP protein isoforms resolved by high-resolution two dimensional (2D) electrophoresis (55) and the apparent lack of a structure-function correlation between its capsid proteins. Indeed, the MVM capsid is composed of VP-1 (83-kDa) and VP-2 (64-kDa) proteins (64), which have identical amino acid sequences, with VP-1 including VP-2 plus a 143-amino-acid N-terminal domain (67, 68), and a common three-dimensional crystal structure of the core of 547 amino acids (3) but which play different biological roles during the infectious cycle. VP-2 is necessary for capsid formation and encapsidation of the viral genome (72, 74), it determines the tropic properties of the capsid (34), and it drives capsid protein oligomers into the nucleus (42), but VP-1 is specifically required for infectivity of virus progeny (72). Moreover, the topology of these polypeptides is not exactly the same in the virions. MVMp DNA-containing virions harbor variable amounts of a third structural polypeptide, VP-3, derived from the cleavage of the VP-2 N-terminal domain during the process of internalization in the infected cell (19, 47, 55). The VP-2 cleavage may be partially mimicked in vitro by digestion of DNA-containing particles with trypsin and to a lesser extent with chymotrypsin (48, 67), but VP-1 is fully resistant. The differential accessibility to proteases of VP-2 in DNA-containing but not in empty particles implies that viral DNA encapsidation must alter the capsid structure to expose the VP-2-processing site (18). However, it remains unclear why the VP-1 region corresponding to the VP-2 N-terminal domain is not externalized in the virions or which role VP-2 cleavage plays in the virus infectious cycle (47, 71).

This report addresses the nature and biological significance of MVMp capsid phosphorylation in vivo. The VP-2 and VP-1 subunits are shown to harbor complex and specific patterns of Ser and Thr phosphorylation when assembled in capsids. A biochemical and genetic analysis was undertaken to map and characterize the most highly phosphorylated peptide of VP-2, the major protein component of the MVMp capsid. We show that three proximate serine residues of the unordered VP-2 N-terminal sequence form the main phosphorylated domain of the MVMp particle, and although they are not required for the externalization and maturation cleavage of this domain, these phosphorylated residues are important to a productive viral life cycle.

MATERIALS AND METHODS

Cell lines and virus. The A9 mouse fibroblast and the NB324K simian virus 40-transformed human newborn kidney cell lines described as hosts for the MVMp strain (66) were maintained in Dulbecco modified Eagle medium (DMEM) supplemented with 5% heat-inactivated fetal calf serum (FCS) (Gibco BRL). Virus stocks of the prototype parvovirus MVMp (20) were prepared in the A9 cell line from infections at low multiplicity, purified by density gradient centrifugation as previously described (56), and stored at −70°C.

Metabolic radiolabeling of virions and capsids. For the production of mature labeled MVM capsids and virions, NB324K cells were seeded at a density of 10,000 cells/cm^2 in 90-mm-diameter dishes and cultured overnight in DMEM supplemented with 5% FCS. The cells were infected at a multiplicity of infection of 10 PFU/cell and labeled from 4 to 48 h postinfection (p.i.) in 3 ml of either

methionine-free DMEM supplemented with 10% normal medium, 10% dialyzed FCS, and 300 μCi of [^{35}S]methionine (Amersham SJ5050) or starved for 4 h in phosphate-free DMEM plus 10% dialyzed FCS and labeled in the same medium with 0.5 mCi of carrier-free [^{32}P]orthophosphate per ml (Amersham PBS13). For immature-virus production, the labeling was carried out for 10 to 16 h p.i. in medium lacking methionine but containing 10% dialyzed FCS, and 200 μCi of [^{35}S]methionine per ml. At the end of the labeling periods, the cells were harvested and processed for purification of MVM particles as described below.

Purification of labeled MVMp particles. Wild-type and mutant virions and capsids labeled with ^{35}S and ^{32}P were purified as previously described (55) with some modifications. Plates containing virus showing cytopathic effect, normally 3 to 4 days p.i., were harvested by direct scraping of the cells into the medium supplemented with protease inhibitors (1 mM phenylmethylsulfonyl fluoride, 10 μg of aprotinin per ml, 10 μg of pepstatin per ml, 10 μg of leupeptin per ml) and phosphatase inhibitors (5 mM NaF, 20 mM β-glycerophosphate), sodium dodecyl sulfate (SDS) was added to 0.2%, and debris was removed by low-speed centrifugation in a Sorvall SS34 rotor (10,000 × g for 15 min at 4°C). For the analysis of immature virions, cell monolayers were washed three times with phosphate-buffered saline at 16 h p.i., and scraped in 50 mM Tris (pH 8.0)–1 mM EDTA–inhibitors as above–0.2% SDS, and DNA was sheared by flushing through a 25-gauge needle. The respective homogenates were centrifuged for 18 h at 16,000 rpm and 15°C in a Beckman SW40 rotor (30,000 × g) through 2 volumes of a 20% sucrose cushion in 50 mM Tris (pH 8.0)–0.1 M NaCl–1 mM EDTA–0.2% SDS. The pellets were resuspended in 1.0 ml per 90-mm dish containing 20 mM Tris-HCl (pH 8), 1 mM EDTA, 0.2% sarcosyl, and the protease and phosphatase inhibitors as above, and clumps were disaggregated by gentle sonication and flushing through a 25-gauge needle. The suspensions were brought to 10 ml of 20 mM Tris (pH 8.0)–1 mM EDTA–0.2% Sarcosyl, adjusted to a density of 1.38 g/ml in CsCl by refractometry, and centrifuged to equilibrium for 42 h at 48,000 rpm and 15°C in a Beckman Ty65 rotor (150,000 × g). Gradients were fractionated and tested for hemagglutination activity with mouse erythrocytes, and the label distribution was determined by scintillation counting. Fractions containing labeled particles with a density corresponding to empty MVM capsids (1.32 g/ml) and to DNA-containing virions (1.39 to 1.41 g/ml) were pooled, extensively dialyzed, and concentrated by ultracentrifugation when required.

Analysis of phosphoamino acids. Purified ^{32}P-labeled MVMp particles were subjected to SDS-polyacrylamide gel electrophoresis (10% polyacrylamide) (PAGE) and the separated proteins were electroblotted onto polyvinylidene difluoride membranes (Immobilon-P; Millipore, Bedford, Mass.). The membranes were exposed for autoradiography, and the identified VP proteins were excised from the membranes with the aid of the film signals. The strip of membrane was rinsed several times with deionized water, and acid hydrolysis was performed in 6 N HCl for 2 h at 110°C in vials purged with nitrogen (31). These conditions were found optimal for release of phosphoamino acids from the proteins with minimal removal of free inorganic phosphate (P$_i$) from phosphoamino acids. Samples were frozen, lyophilized in a Speed-Vac concentrator (Savant, Hicksville, N.Y.), and resuspended in 5 μl of pH 1.9 buffer (0.58 M formic acid, 1.36 M glacial acetic acid) containing 0.3 μg each of phosphoamino acid standards (Sigma). Samples were applied to 20- by 20-cm thin-layer chromatography (TLC) plates (Merck, Darmstadt, Germany) and electrophoresed in pH 1.9 buffer for 90 min at 1.5 kV (Multiphor; Pharmacia-LKB) with cooling at 10°C. Second-dimension electrophoresis was for 30 min at 1.5 kV in pH 3.5 buffer (0.5% pyridine, 0.87 M glacial acetic acid). The dry plates were exposed for autoradiography to X-ray films at −70°C with an intensifying screen, and the phosphoamino acids markers were visualized by spraying with 0.25% ninhydrin solution in acetone.

2D phosphopeptide analysis. Proteins resolved by SDS-PAGE (10% polyacrylamide gels) were transferred onto a nitrocellulose membrane (0.45 μm pore size, BA85; Schleicher & Schuell) with an electrophoretic transfer system in 40 mM glycine–50 mM Tris base–0.02% SDS–20% methanol for 60 min at 100 V, and the positions of the VP proteins were identified by autoradiography with X-ray films. Protein bands were excised from the membranes, and the pieces of membrane were soaked for 30 min at 37°C in 0.5% polyvinylpyrrolidone-360 (Sigma) in 100 mM acetic acid and extensively washed with deionized water. Following a previously described method (12), samples were digested with 10 μg of N-tosyl-L-phenylalanine chloromethyl ketone (TPCK)-trypsin (sequencing grade; Boehringer) in 50 μl of 50 mM NH$_4$HCO$_3$ (pH 8.0) for 5 h at 37°C, and then an additional dose was added and incubation was continued overnight at the same temperature. The tryptic peptides were oxidized with performic acid for 60 min on ice, diluted in deionized water, concentrated in a centrifugal vacuum concentrator, cleaned by repeated lyophilization, resuspended in 5 μl of buffer (pH 1.9), and applied to 20- by 20-cm TLC plates. Two-dimensional analysis was carried out by electrophoresis in buffer (pH 1.9) at 1.0 kV for 30 min under cooling at 10°C for the first dimension and by ascending chromatography orthogonal to the first dimension in 38% n-butanol–25% pyridine–7.5% acetic acid for the second dimension. The plates were exposed to X-ray films in the presence of an intensifying screen at −70°C or to a radioanalytic imaging system (Fujix BAS 1000; Fuji).

For secondary protease digestions of isolated phosphopeptide B, the exact position of the peptide was localized in the ^{32}P-fingerprint with the aid of the film and the peptide was scraped off the plates and dissolved in 20 μl of pH 1.9 buffer.

The matrix was washed several times with this buffer and water and centrifuged, and the supernatants were collected and lyophilized. Equal amounts of purified peptide B were resuspended in the appropriate protease buffers as follows: α-chymotrypsin (Boehringer), 50 mM NH_4HCO_3 (pH 8); thermolysin (Sigma), 50 mM NH_4HCO_3 (pH 8)–1 mM $CaCl_2$; endoproteinase Glu-C (V8; Boehringer), 50 mM sodium phosphate buffer (pH 7.8); and proteinase K (Merck), 50 mM Tris (pH 8)–10 mM NaCl–10 mM EDTA. Samples were incubated overnight with 10 μg of each protease at 37°C, except for thermolysin, which was incubated at 55°C. The digestion products were lyophilized, applied to TLC plates, and electrophoresed in one dimension in pH 1.9 buffer at 1 kV for 30 min. The dried plates were exposed for autoradiography in a phosphorimager as above.

Construction and growth of site-directed MVMp mutants. Mutations were created by oligonucleotide-directed mutagenesis by the procedure of Kunkel (36), using the M13mp18 phage vector. Mutations were transferred to the MVMp genome by exchanging the HinDIII-HinDIII (nucleotides 2795 to 2858) of the wt infectious plasmid pMM984 (44) for the mutated fragment. The introduced amino acid changes numbered from the start of VP-2, the nomenclature of the virus mutants (in parentheses), and the mutated nucleotide positions in the MVM genome (7), respectively, were as follows: amino acid Ser-2 to Gly (S2G), nucleotide AGT (nt 2798) to GGT (nt 2800); Ser-6 to Gly (S6G), nucleotide AGC (nt 2810) to GGC (nt 2812); Ser-10 to Gly (S10G), nucleotide AGC (nt 2821) to GGC (nt 2823); Ser-16 to Gly (S16G), nucleotide TCA (nt 2839) to GGA (nt 2841); Ser-2 and Ser-6 to Gly (S2, 6G), nucleotide AGT AGC to GGT GGC; Ser-2, Ser-6, Ser-10, and Ser-16 to Gly (4S/G), nucleotides AGT AGC AGC TCA to GGT GGC GGC GGA. Oligonucleotides used for mutagenesis were: CCATGGGTGATGGCACC for the S2G mutant, GATGGCACCGGCC AACC for the S6G mutant, CCTGACGGCGGAAACGC for the S10G mutant, and CCACGGAGCTGCAAGAG for the S16G mutant. To introduce two or multiple mutations, the required oligonucleotides were used in combination. Mutations were verified in the double-stranded plasmid DNA preparations to be used for cell transfection by sequencing by the dideoxynucleotide-mediated chain termination method incorporating [^{35}S]dATP with T7 DNA polymerase (Pharmacia). Oligonucleotides were purchased from Isogen Bioscience BV (Maarssen, Holland).

To obtain mutant viruses for protein labeling of MVMp particles and for phenotypic characterization, the corresponding plasmid amplified in the JC8111 bacterial strain that preserves the viral hairpins necessary for replication (10) (and is enriched in supercoiled forms by chromatography [Qiagen]) was transfected in growing NB324K cells by electroporation. Usually 6×10^6 cells were electroporated with 20 μg of plasmid as previously described (41), seeded at low density, and cultured for 48 h postelectroporation. Cell monolayers were washed and scraped in phosphate-buffered saline, the intracellular virus was released by three cycles of freezing-thawing and low-speed centrifugation, and virus titers were estimated by a plaque assay on NB324K cells. Viral stocks were prepared by infecting 8×10^6 NB324K cells at low multiplicity of infection (0.01 PFU/cell) and culturing them just until the appearance of an incipient cytopathic effect (usually 72 h p.i.) to minimize the emergence of secondary mutations. Viruses devoid of empty capsids were then purified by centrifugation through a sucrose cushion and CsCl equilibrium centrifugation as described above and stored at −70°C. Finally, the introduced point mutations were confirmed in the viral preparation by PCR amplification of a region of the MVM genome expanding the VP-2 N-terminal region and sequenced by the dideoxynucleotide chain termination method.

Trypsin digestion of MVMp particles. For digestion of purified wt capsid and DNA-containing virions labeled with either [^{35}S]Met-[^{35}S]Cys or [^{32}P]orthophosphate as outlined in Fig. 3B, about 0.1 μg of purified particles was incubated with 2 μg of trypsin (sequencing grade; Boehringer) in 50 μl of 50 mM Tris-HCl (pH 8.8)–5 mM EDTA for 2 h at 37°C. In the quantitative analysis of VP externalization in wt and mutant viruses (see Fig. 7C), 0.01 μg of ^{35}S-labeled DNA-containing particles harvested and purified at 16 h p.i. was digested under the same conditions with the indicated low doses of trypsin for 30 min at 37°C.

Phenotypic analyses of virus phosphorylation mutants. The number of particles in the purified virion samples to be used for specific infectivity studies was estimated by measuring the total amount of VP proteins by SDS-PAGE (10% polyacrylamide) with Coomassie blue staining, using a solution of bovine serum albumin as standard, and considering a molecular weight of 5.5×10^6 for the MVMp particle (60). Values were further validated in a hemagglutination assay with mouse erythrocytes performed in parallel using serial twofold dilutions. The infectivity titers of the diverse virus preparations were determined by plaque assays in the NB324K cell line (27). In the test of infection initiation (see Fig. 8C and D), monolayers of NB324K cells were inoculated with a normalized number of virions, neutralizing antibody was added at 6 h p.i. to block reinfections, and the number of infected cells was determined by indirect immunofluorescence (IF) with a rabbit MVM capsid antiserum as described previously (41).

RESULTS

The VP-1 and VP-2 structural proteins of the parvovirus MVMp are phosphorylated in serine and threonine residues in vivo. The extension of phosphorylation of the MVMp struc-
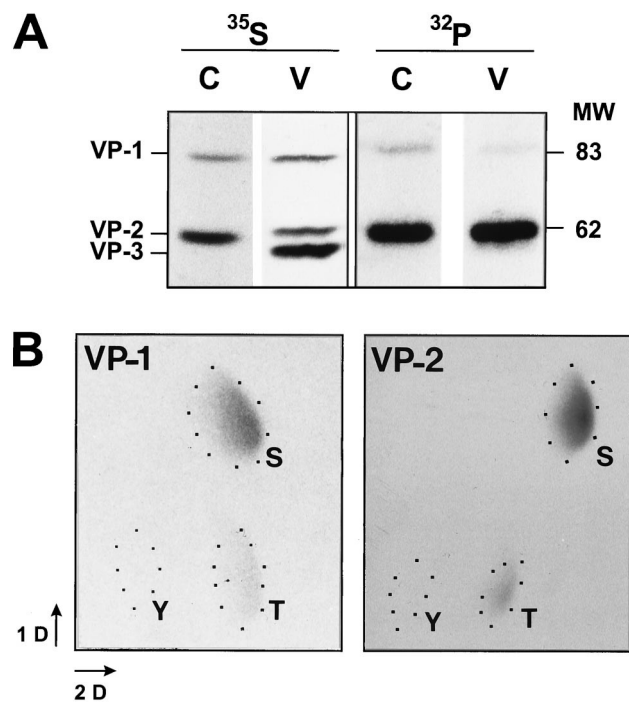

FIG. 1. Phosphorylation of the MVMp structural proteins assembled in particles. (A) SDS-PAGE of MVMp empty capsids (lanes C) and DNA-full virions (lanes V) purified from infected NB324K cells labeled with [^{35}S]Met-[^{35}S]Cys or [^{32}P]orthophosphate. Gels were fixed and exposed to autoradiography for 48 h (^{35}S) or blotted to nitrocellulose and the filter was exposed 48 h at −70°C with an intensifying screen (^{32}P). The positions of the MVMp structural proteins are indicated to the left, and their approximate molecular weights (MW) are given to the right in kilodaltons (B) Phosphoamino acid composition of the VP-1 and VP-2 proteins of MVMp capsid. Shown are autoradiograms of thin-layer 2D electrophoresis of phosphoamino acid analysis of labeled VP-1 and VP-2. The regions circled by dashed lines indicate the positions where the phosphoamino acid markers migrated. S, phosphoserine; T, phosphothreonine; Y, phosphotyrosine; 1D, first dimension; 2D, second dimension.

tural proteins assembled in capsids and virions produced in permissive NB324K cells was compared in ^{32}P-labeled particles purified from infected cultures. The VP-1 and VP-2 proteins were significantly phosphorylated in both types of particles (Fig. 1A). The degree of phospho-label in these protein subunits, measured as the ^{35}S/^{32}P ratio of the bands in the gels, was estimated proportional to their relative abundance in the MVMp particles, although a clear VP-1 signal in the virion samples required overexposure of the gels. In contrast, the VP-3 protein, which is a highly abundant polypeptide in mature virions recovered at late times p.i. (Fig. 1A, left), was barely detected in the autoradiograms of the phosphorylation experiments (Fig. 1A, right). A similar uneven distribution of the phosphate substituent in the structural proteins of MVMp particles was previously observed in the infection of A9 fibroblast cells (55).

The nature of the phospho-substituent in MVMp structural proteins was determined by performing 2D phosphoamino acid analysis with gel-isolated radiolabeled VP-1 and VP-2 proteins of purified capsids. The ^{32}P-labeled amino acids from both VP-1 and VP-2 capsid proteins comigrated with authentic phosphoserine and phosphothreonine standards (Fig. 1B). The label was mainly in phosphoserine and was severalfold lower in phosphothreonine (Fig. 1B). There was no trace of phosphotyrosine and no significant amount of inorganic free phosphate (P_i) under the adopted conditions of acid hydrolysis (see Ma-
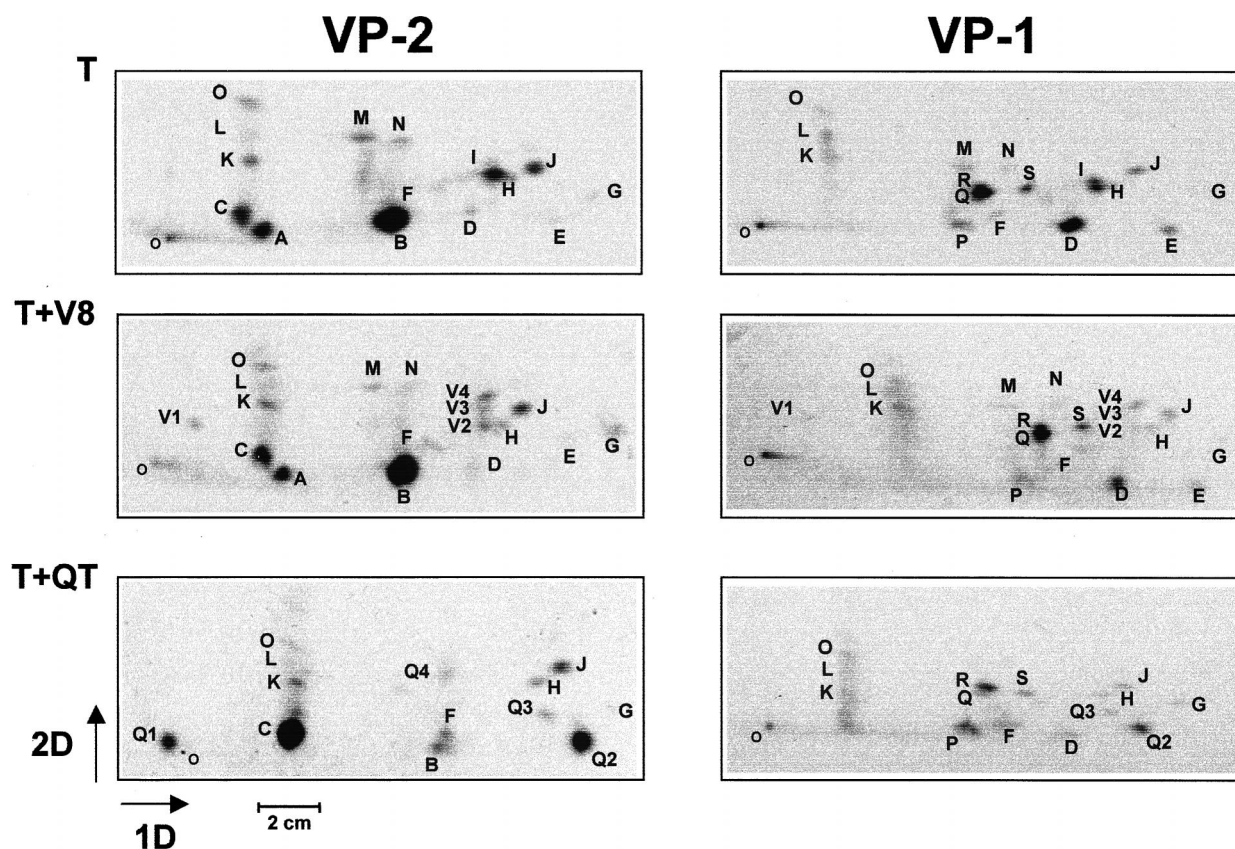
FIG. 2. 2D phosphopeptide maps of parvovirus MVMp capsid proteins. VP-1 and VP-2 proteins isolated from purified ^{32}P-labeled MVMp capsids were digested with proteases and subjected to two-dimensional TLC analysis. Shown are the phosphopeptide maps from trypsin (T), trypsin-plus-endoproteinase-V8 (T+V8), and trypsin-plus-chymotrypsin (T+QT) digestions. The primary VP-2 tryptic peptides are alphabetically designated in the autoradiograms according to their 2D migration (left to right starting from the bottom of the plates), and this nomenclature is maintained for the peptides shared with VP-1 (D to O). Specific VP-1 peptides were designated P to S. Peptides arising from subsequent digestions were identified by comparative analysis of superimposed films and are designated by the initial letter of the secondary protease used (V, V8; Q, chymotrypsin) followed by an arbitrary number. Plates were exposed to autoradiography with an intensifying screen for 4 to 7 days at −70°C. Only the areas of the plates where the phosphopeptides migrated are shown. 1D, first dimension; 2D, second dimension; o, origin. The resolution is indicated by the scale bar.

terials and Methods). Therefore, the phospho-substituent in the capsid proteins of MVMp is found as conventional phosphoamino acids, i.e., serine and threonine the main phosphate acceptors.

The VP-1 and VP-2 subunits of the MVMp capsid show complex and different patterns of phosphorylation. An estimation of the number and distribution of the phosphorylated serine and threonine residues along the amino acid sequences of the MVMp capsid subunits was investigated by 2D TLC of the phosphopeptides resulting from single and combined protease digestions of radiolabeled VP-1 and VP-2 proteins. The VP-2 tryptic map was resolved as a highly reproducible pattern of 15 unevenly phosphorylated peptides (Fig. 2, panel T, top left) that were designated A to O. The B peptide harbored more than 10 times the amount of label of any of the others, whereas four peptides (A, C, I, and J) showed intermediate phosphorylation levels and the rest were weakly phosphorylated. Unevenly labeled phosphopeptides may result from the clustering of phosphorylated residues as well as from different degrees of phosphate incorporation at precise amino acid positions. To gain some insight into the characteristics of the uneven phosphate distribution in VP-2 the tryptic phosphopeptides were subjected to secondary digestion with other proteases. The digestion of VP-2 tryptic peptides with protease

V8 gave rise to four new phosphopeptides (V1 to V4) and the loss of most of the label in peptide I (Fig. 2, panel T+V8, middle left). Since the rest of the pattern remained unchanged, peptide I should contain at least three phosphorylated residues alternating with V8 protease cleavage sites. This evidence raised to 18 the minimal number of phosphorylated residues in the VP-2 subunits forming the MVMp capsids. In contrast, most VP-2 tryptic phosphopeptides, including major ones (A, B, and I), were susceptible to chymotrypsin digestion (Fig. 2, panel T+QT, bottom left), although peptide C and some minor ones (peptides F, G, H, J, K, L, O) seemed not to contain cleavage sites for this protease. The digestion with chymotrypsin gave rise to the appearance of some reproducible phosphopeptides (Q1 to Q4).

The VP-1 tryptic map showed an overall resemblance to that of VP-2, since the 2D migration of the D to O peptides was conserved (Fig. 2, top right), illustrating that the entire VP-2 amino acid sequence is included in VP-1. However, some clear differences were manifested between the two fingerprints: (i) the three major VP-2 phosphopeptides (A, B and C) were absent in VP-1, (ii) peptide D became a major peptide in VP-1, and (iii) four new phosphopeptides (designated P to S) were specific for the VP-1 tryptic map. These conclusions were further supported by the digestions of the VP-1 tryptic phos-

phopeptides by additional proteases. First, as in VP-2, only the VP-1 I peptide was cleaved to the V1 to V4 peptides by the V8 protease (Fig. 2, middle right), and the D, E, I, M, and N peptides, but not the F, G, H, J, K, L, and O peptides, were cut with chymotrypsin (Fig. 2, bottom right). Second, the VP-1-specific phosphopeptides behaved differently from the A and B major VP-2 peptides, since only the Q peptide, but not the P, R, and S peptides, was digested with chymotrypsin. This difference may account for the fact that the leftward-moving Q1 peptide arising in the trypsin-plus-chymotrypsin digestion of VP-2 was not present in the corresponding VP-1 fingerprint (Fig. 2, bottom panels). In summary, this analysis demonstrated that the VP-2 and VP-1 protein subunits forming the MVMp capsid harbor at least 18 phosphorylation sites. It is noteworthy that the major ones are distinct and specific for either type of capsid subunit yet most weakly phosphorylated sites are shared by both polypeptides.

The major phosphorylation domain of the MVMp particle localizes within the VP-2 N-terminal sequence externalized in DNA-containing virions. Our study next focused on the tryptic peptide B of VP-2, the main phosphopeptide of the major protein component of the MVMp capsid. With the aim of localizing peptide B in the VP-2 sequence, the tryptic maps of VP-2 and VP-3 subunits isolated from [^{35}S]Met-[^{35}S]Cys-labeled purified virions were compared. VP-3 is derived from VP-2 by a cleavage that removes about 20 amino acids of its N-terminal sequence (48, 67); therefore, comparison of the fingerprints of these polypeptides could allow the identification of the tryptic peptides belonging to the VP-2 N terminus. In our TLC system of analysis, the 2D tryptic maps of [^{35}S]Met-[^{35}S]Cys-labeled VP-2 and VP-3 were undistinguishable except for one single peptide resolved in VP-2 but clearly missing in the VP-3 fingerprint (Fig. 3A). Interestingly, this ^{35}S-peptide migrated in the TLC plates at a position matching that of phosphopeptide B in the VP-2 fingerprint (Fig. 2). This result suggested that phosphopeptide B lies in the amino-terminal domain of VP-2 processed during virus maturation in culture.

The VP-2 N-terminal sequence is externalized outside the protein shell in DNA-containing virions, which allows its in vitro cleavage with trypsin (64, 68, 71). We used this test to further study whether phosphopeptide B was the VP-2 N-terminal domain. As expected, only in DNA-containing virions could a high proportion of the ^{35}S-labeled VP-2 subunits be cleaved with trypsin to VP-3 (Fig. 3B). Accordingly, the ^{32}P label incorporated in the VP-1 and VP-2 subunits of purified empty capsid was fully resistant to high doses of trypsin at 37°C, since no loss of ^{32}P signal was found even after prolonged incubation times (Fig. 3B, left). In the purified DNA-containing virions, the ^{32}P label was found mainly in the VP-2 polypeptide as well, but here the trypsin digestion removed most of it (Fig. 3B, right). In addition, the otherwise barely detected VP-3 became a major phosphoprotein of the digested virions. However, the ^{32}P signal present in VP-3 upon digestion did not account for the major loss from VP-2, and thus most of the VP-2 phospholabel must reside in the peptide cleaved off by trypsin. Taken together, these results mapped the highly phosphorylated peptide B to the amino-terminal domain of VP-2.

The three distal serine residues of the VP-2 N terminus are phosphorylated in the MVMp particle. The prominent phosphorylation of the VP-2 N-terminal domain prompted us to investigate the nature and localization of the phosphate substituent in peptide B. For this purpose, peptide B extracted from TLC plates of the ^{32}P-labeled VP-2 tryptic fingerprint (Fig. 2) was subjected to phosphoamino acid analysis. As shown in Fig. 4A, phosphoserine was the only type of phos-
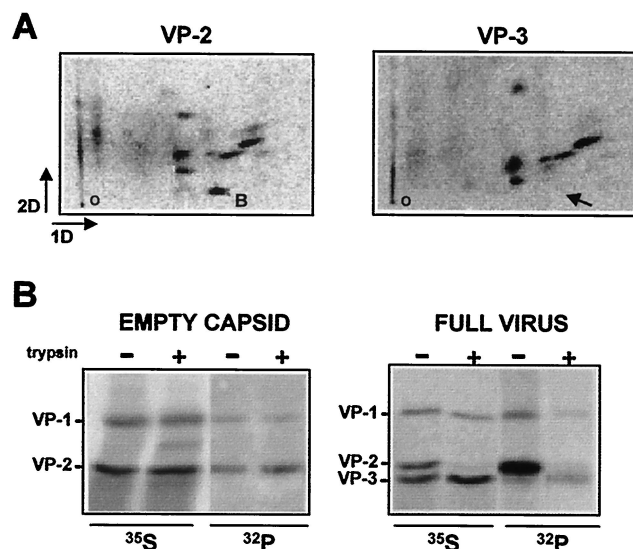

FIG. 3. Analysis of phosphopeptide B localization in VP-2. (A) 2D tryptic maps of [^{35}S]Met-[^{35}S]Cys-labeled VP-2 and VP-3 proteins isolated from purified MVMp virions. The dried TLC plates were exposed for autoradiography in a Fujix Bas 1000 phosphorimager (Fuji) for 5 days. The arrow indicates the absence in VP-3 fingerprint of VP-2 peptide B. 1D, first dimension; 2D, second dimension; o, origin. (B) In vitro trypsin digestion of MVMp particles. Purified ^{35}S- and ^{32}P-labeled MVMp empty capsids and DNA-containing viruses were digested (+) with an excess of trypsin for 2 h at 37°C or not digested (−), and the samples were resolved by SDS-PAGE (10% polyacrylamide) and blotted to nitrocellulose membranes, and the filters were exposed for autoradiography in a phosphorimager for 2 days. The positions of the three MVMp structural proteins are indicated.

phoamino acid found in peptide B. Besides this finding, additional phosphorylations of the VP-2 N terminus distinct from conventional phosphoamino acids were considered. Peptide B digested into its amino acids with proteinase K was quantitatively analyzed by thin-layer electrophoresis to find the proportion of the phospholabel corresponding to phosphoserine. The phospholabel from peptide B digestion migrated as phosphoserine (Fig. 4B), indicating that the nature of peptide B phosphorylation was exclusively amino acidic and ruling out any significant contribution of other type of phospho-substituent in this region of VP-2.

Initial attempts to fractionate the VP-2 phosphopeptides by reverse-phase high-performance liquid chromatography were judged unsatisfactory due to the presence of weakly phosphorylated peptides demonstrable in overexposed TLC fingerprints of the fractions. Thus, the mapping of the phosphorylated serine residues in peptide B was next attempted by a method that combined chemical and genetic analysis. The four serines contained within the VP-2 N-terminal tryptic peptide at amino acid positions 2, 6, 10, and 16 of the MVMp genome (7) were changed to glycines in an infectious MVMp plasmid (44). Viruses with point mutations at the respective serines (designated S2G, S6G, S10G, and S16G), as well as a multiple-mutant virus harboring all four serine residues changed to glycine (4S/G), could be recovered in sufficient amount from transfected permissive NB324K cells and were purified on CsCl gradients (see Materials and Methods). These viruses were subsequently used for infection, and radiolabeled empty capsids were prepared to determine the phosphorylation pattern of the mutant VP-2 subunits by 2D tryptic phosphopeptide analysis. The 4S/G mutant capsid lacked ^{32}P-labeled peptide B but contained the rest of the phosphopeptides characteristic of
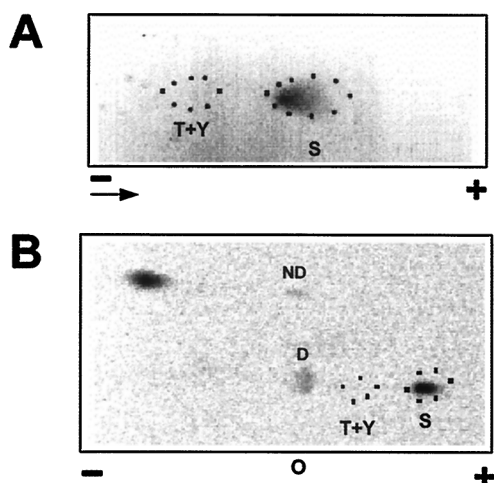
FIG. 4. The VP-2 N-terminal domain is phosphorylated exclusively in serine residues. (A) Phosphoamino acid analysis of peptide B. Autoradiography of acid hydrolysis of peptide B subjected to one-dimensional thin-layer electrophoresis is shown. The positions where markers migrated are encircled by dotted lines. T+Y, phosphothreonine plus phosphotyrosine; S, phosphoserine. (B) Quantitative analysis of the proportion of the peptide B phospho-label corresponding to phosphoamino acids. ND, undigested peptide B; D, peptide B digested to amino acids with proteinase K. Markers and electrophoretic conditions were as in panel A. Both type of analyses were performed with approximate 200 cpm of pure phosphopeptide B, and the plates were exposed for autoradiography in a phosphorimager (Fuji) for seven days. o, origin.

FIG. 5. Several serine residues are phosphorylated in the VP-2 N-terminal domain. The figure shows VP-2 tryptic maps of ^{32}P-labeled MVMp capsids purified from the infection of NB324K cells with the indicated virus mutants. Note the absence of phosphopeptide B in the autoradiogram of the multiple mutant 4S/G (arrowhead) and its comparable signal in the single-site mutants shown (S2G and S10G). Plates were exposed in a phosphorimager (Fuji) for 4 days. 1D and 2D, first (electrophoresis) and second (chromatography) dimensions, respectively; o, origin.

VP-2 (Fig. 5, bottom), in agreement with the exclusive phosphoserine content of peptide B described above. Unexpectedly, however, the S2G and S10G mutants (Fig. 5), as well as any of the other single mutants (data not shown), harbored similar VP-2 phosphorylation patterns, with peptide B represented at high levels. This study revealed that several serine residues may act as phosphate acceptors in this region of VP-2.

Localization of the several phosphoserine residues at the VP-2 N terminus was investigated by digesting purified phosphopeptide B from wt and single-mutant viruses with a panel of sequence-specific proteases and resolving the digestion products by one-dimensional thin-layer electrophoresis (Fig. 6). The amino acid sequence of the tryptic peptide B contains two potential cleavage sites for α-chymotrypsin, two for endoproteinase V8, and one for thermolysin (Fig. 6, bottom left). Chymotrypsin cut wt peptide B to give one single leftward-moving phosphopeptide with a relative mobility lower than that of the undigested sample, and thermolysin produced a single rightward-moving phosphopeptide (Fig. 6, top left). The latter result indicated that phosphorylation of wt peptide B must occur either at Ser 16 or in the group formed by Ser2, Ser6, and Ser10. Interestingly, the thermolysin peptide remained uncut after chymotrypsin incubation, indicating that phosphorylation protected at least one of the two chymotrypsin recognition sites against the cleavage. Indeed, the occurrence of a protection phenomenon was strengthened by the full resistance of wt peptide B to a high dose of V8 protease, which further suggested that phosphorylations at positions near the two V8 cleavage sites at positions D3 and D9 (Fig. 6, left) were likely. The S16G mutant peptide showed a pattern of susceptibility to proteases identical to that of the wt (Fig. 6, bottom right), ruling out Ser16 as a phosphorylation site in the wt VP-2 protein. Furthermore, this mutant peptide showed that chymotrypsin cleaved only at position H15 and not at position Q7, and thus the latter site must be protected against this protease by some proximate phosphate radicals. The maintenance of
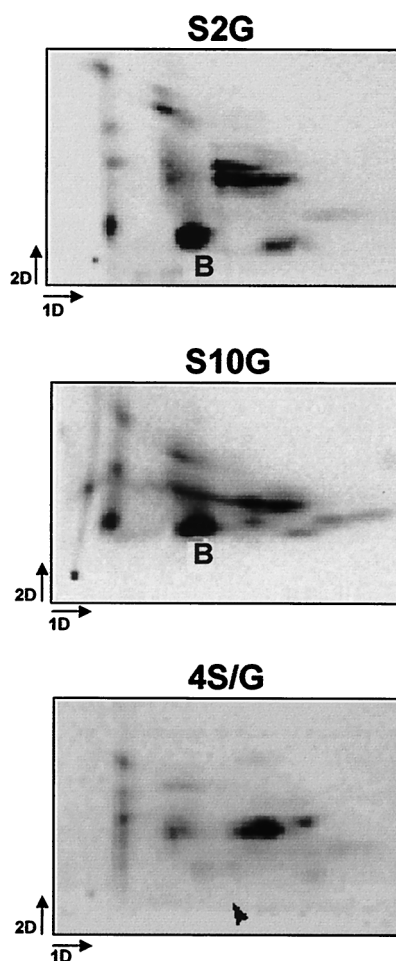
the same pattern of protease susceptibility in the S10G mutant phosphopeptide as well (Fig. 6) did indicate that either Ser2 or Ser6, or both, must be phosphorylated in the wt VP-2. In contrast to this behavior, the S2G mutant peptide could easily be digested with V8 (Fig. 6, central panel), pointing to Ser2 as a phosphorylated residue normally protected against V8 activity in the wt peptide B. Moreover, the fact that two phosphopeptides were clearly resolved in the V8 digestion of this mutant allowed the identification of Ser6 and Ser10 as the two other phosphorylated positions in the wt peptide. This conclusion was fully supported by the analysis of the S6G mutant peptide, in which the release of protection against V8 activity validated Ser6 as a phosphorylation site, and the production of two more V8 phosphopeptides here also indicated that two more positions, namely, Ser2 and Ser10, must also be phosphorylated. Collectively, this analysis allowed us to assign Ser2, Ser6, and Ser10 as the preferentially phosphorylated amino acid positions in the VP-2 protein subunits forming the MVMp capsid.
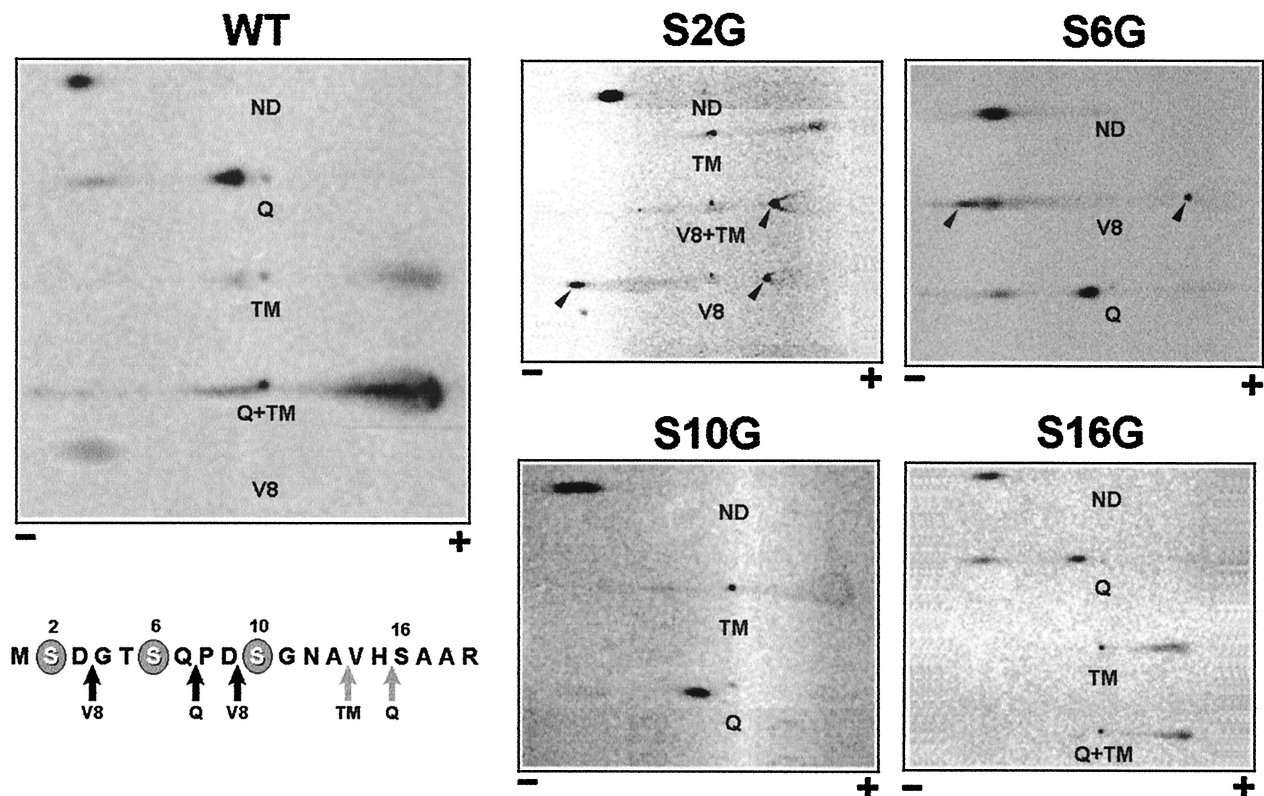
FIG. 6. Mapping the phosphorylated serine residues within the VP-2 N-terminal domain. Peptide B isolated from VP-2 phosphopeptide maps of wt and mutant capsids (Fig. 2 and 5) were incubated with the indicated proteases, and the digestion products were resolved by one-dimensional thin-layer electrophoresis. Samples were applied at the center of the TLC plates. Arrowheads in the panels point to mutant phosphopeptides not seen in the corresponding protease digestions of wt peptide B. Abbreviations: ND, undigested peptide B; Q, α-chymotrypsin; TM, thermolysin; V8, endoproteinase Glu-C. The amino acid sequence of wt tryptic peptide B is shown at the bottom left with the phosphoserine residues determined in this work encircled in bold and the protease cleavage sites indicated by arrows. Black arrows: protease recognition sites refractory to cleavage; grey arrows, cleavage sites accessible to proteases. The single-letter code for the amino acids is as follows: A, Ala; D, Asp; E, Glu; G, Gly; H, His; M, Met; N, Asn; P, Pro; Q, Gln; R, Arg; S, Ser; T, Thr; V, Val.

VP-2 maturation cleavage in the absence of N-terminal phosphorylation. A high proportion of the VP-2 subunits of the DNA-containing particles, but not the VP-1 subunits, are cleaved at their N-terminal domain in a process accompanying MVM entry into cells (19, 47, 55). Since the VP-2-specific phosphopeptide B localizes at this cleaved domain, we hypothesized that the negative charges of the three phosphoserine residues would determine an electrostatic repulsion with the packaged DNA backbone, leading to the externalization of this domain and thus facilitating its processing. To explore this idea, the extension of natural VP-2 processing in virions grown in culture and the accessibility of the VP-2 N-terminal sequence to trypsin cleavage in vitro were compared between wt and mutant viruses. ^{35}S-labeled virions obtained at 72 h p.i. from NB324K cultures showing extensive cytopathic effect were purified and their protein composition was analyzed by SDS-PAGE. The 4S/G mutant, lacking phosphopeptide B (Fig. 5), showed a relative abundance of VP-3 similar to the wt virions (Fig. 7B), as did the S6G and S2G mutants with genetic changes at single serine residues (data not shown). This result indicated that VP-2 could be quantitatively cleaved during virus progression in culture in the absence of phosphorylation at its N-terminal domain. To study whether the VP-2 processing occurring in vivo could be explained by the externalization of the VP-2 unphosphorylated N-terminal domain, mutant and wt virions were analyzed for VP-2 susceptibility to trypsin cleavage in vitro (48, 67). To minimize natural VP-2 process-

ing, intracellular wt and 4S/G mutant viruses were harvested at 16 h p.i. and purified. These immature viruses incubated with a series of low doses of trypsin showed a similar N-terminal accessibility of their VP-2 subunits to trypsin cleavage, as judged by the comparable VP-2/VP-3 ratio found in the samples throughout the assay (Fig. 7C). Therefore, these in vivo and in vitro studies indicated that serine phosphorylation at the VP-2 N-terminal domain is dispensable for its externalization in the MVMp particles containing the encapsidated virus genome.

Serine phosphorylation at the VP-2 N-terminal domain plays an important role in the MVMp life cycle. To analyze the biological function of VP-2 N-terminal phosphorylation in MVMp infection, the specific infectivities of the phosphorylation mutants and wt viruses were quantitatively compared in a plaque assay. Monolayers of permissive NB324K cells were incubated with viral inocula normalized for the number of virion particles (see Materials and Methods), and the number and size of the plaques were scored after 6 days. wt virions formed an average of 20 plaques per 10^5 inoculated particles (Fig. 8A). However, this value was close to half the wt value for the S2G mutant, three-quarters of the wt value for the S6G and S10G (data not shown) mutants, 1/10 of the wt value for the S2,6G double mutant, and as little as 1/20 of the wt value for the 4S/G mutant (Fig. 8A). Correspondingly, the plaque sizes of the S6G and S10G mutants were similar to those of the wt peptide, but the S2G and 4S/G mutants showed significantly
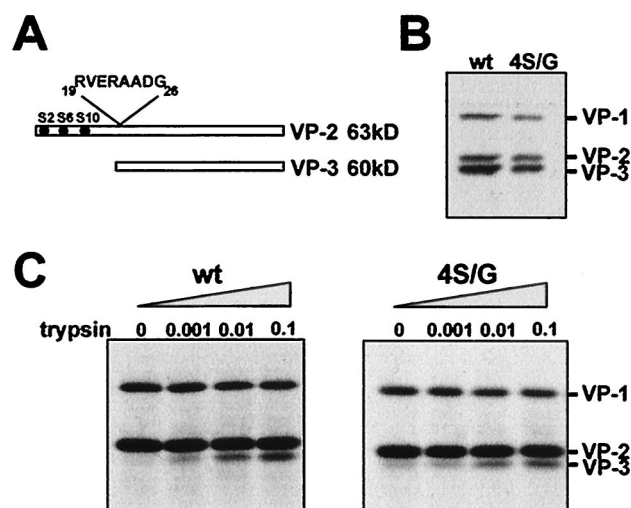
FIG. 7. VP-2 to VP-3 conversion in MVMp virus lacking VP-2 N-terminal phosphorylation. (A) Scheme of VP-2 and VP-3 proteins of MVMp with the trypsin-sensitive sequence (64, 71) and the three mapped VP-2 phosphoserine residues highlighted. (B) SDS-PAGE of ^{35}S-labeled structural proteins of wt and 4S/G mutant virions purified from NB324K cultures at 72 h p.i., showing extensive processing of the VP-2 subunits. (C) Quantitative analysis of VP-2 exposure in immature viruses. ^{35}S-labeled virions (0.01 μg) purified at 16 h p.i. were digested with the indicated amounts of trypsin (in micrograms) for 30 min at 37°C and analyzed by SDS-PAGE. The position of the VP-3 protein is indicated. A total of 500 cpm was loaded per sample, and exposure was for 4 days in a Fujix Bas 1000 phosphorimager (Fuji). The amino acid code is as in Fig. 6.
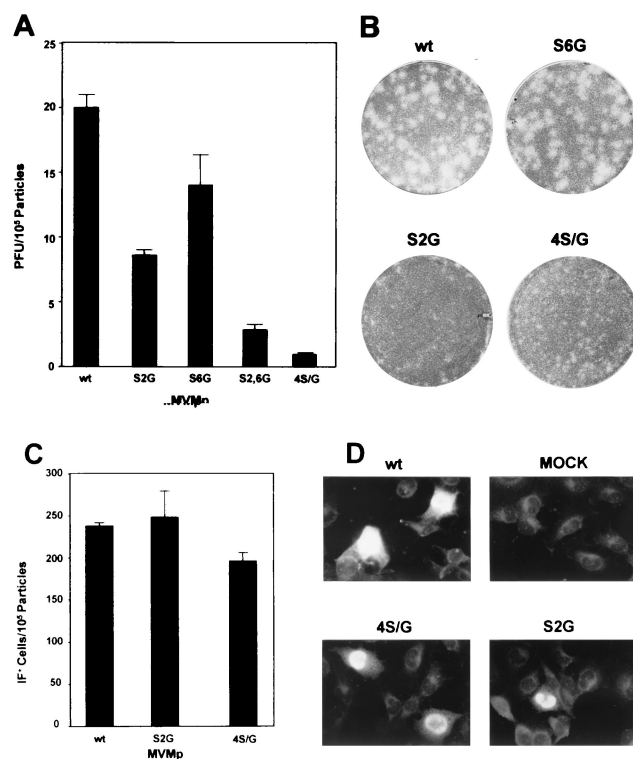

FIG. 8. Phosphorylation of the VP-2 N terminus is required late in the MVMp infection cycle. (A) Plaque-forming capacity of wt and VP-2 phosphorylation mutants. Monolayers of NB324K cells were inoculated with serial dilutions of the indicated viruses and the number of plaques was scored from duplicate plates. Bars represent the mean and standard error of the mean from three independent experiments. (B) Plaque morphology of MVMp viruses in NB324K cells. Plates were developed 6 days after inoculation. Examples of viruses with normal (wt and S6G) and small (S2G and 4S/G) plaque sizes are shown. (C) Assessment of the capacity of the mutant viruses to initiate infection. NB324K cells were inoculated with normalized amounts of purified virus particles, and the number of positive cells for capsid protein synthesis was determined by IF at 24 h p.i. The mean numbers of scored cells and standard errors of the mean from three experiments are shown. (D) Subcellular localization of the synthesized capsid proteins. NB324K cells were inoculated with the indicated viruses and stained by IF at 24 h p.i. with an MVMp capsid antiserum.

smaller plaques (Fig. 8B). This reduced plaque-forming capacity indicated a hampered life cycle in MVMp mutants with altered or lacking VP-2 N-terminal phosphorylation. To carry out a preliminary investigation of the stage of the MVMp life cycle at which the functions of these VP-2 phosphorylations were required, the capacity of the mutant virions to initiate infection was evaluated by determining the synthesis and subcellular localization of the capsid proteins by indirect IF of the inoculated cells. In a single round of infection, wt MVMp produced more than 200 VP-expressing cells per 10^5 inoculated virions, and this number was not significantly reduced in the inoculations with S2G and 4S/G virions (Fig. 8C), the mutants with the most altered phenotype in the plaque assay (Fig. 8A and B). Moreover, the IF staining of the infected cells demonstrated an efficient nuclear targeting of the synthesized wt and mutant capsid polypeptides (Fig. 8D). In agreement with this, these viruses induced similar levels of capsid protein synthesis as measured by SDS-PAGE analysis of ^{35}S-labeled VP proteins (data not shown). These studies indicated that VP-2 N-terminal phosphorylation is not required for the initiation of MVMp infection leading to the synthesis and nuclear translocation of VP proteins but is required for efficient virus plaque formation.

DISCUSSION

Viral capsids are metastable macromolecular complexes required for completion of the viral life cycle inside and outside cells. It is known that capsid functions may be regulated by phosphorylation for some viruses (32, 34, 40), and that some phosphorylation sites are important for polyomavirus assembly (24, 26, 39), but precise data on the distribution and roles of phosphorylation sites in the capsid subunits of icosahedral viruses are still very limited. This report shows for the first time the chemical nature and major characteristics of capsid phosphorylation of a member of the *Parvoviridae* family, MVMp, the prototype strain of the species member of the genus *Parvovirus*. We undertook a systematic phosphorylation analysis of the two types of protein subunits (VP-1 and VP-2) of purified MVMp particles radiolabeled during the infection of susceptible cells, with the aim of increasing our knowledge of MVMp biology and showing that MVMp is a useful model for other icosahedral viruses.

Complex and differential phosphorylation of MVMp capsid proteins in vivo. The capsid proteins of small DNA viruses seem to harbor different types of posttranslational modifications. In the better-characterized polyomavirus system, about six species of VP1, the major protein component of the capsid, were resolved by 2D gel electrophoresis (24, 26) but only the three minor more acidic species were phosphorylated (4, 11). Phosphorylation alone could not explain the heterogeneity of polyomavirus VP1, since the acidic species were identical in their phosphorylation state (11). For the MVMp VP-2 major capsid protein as well, the six neutral protein subtypes resolved by 2D isoelectric focusing could not be justified by their apparent degree of phosphorylation (55). In addition, the large number of phosphopeptides present in VP-2 (Fig. 2), discussed

below, lends further support to the notion that a posttranslational modification other than conventional phosphorylation must be incorporated in the VP-2 subunits for the six protein subtypes to form. Thus, the biochemical basis for the heterogeneity of the MVMp and polyomavirus major capsid proteins in gels remains unclear.

In this work, the VP-1 and VP-2 structural proteins of MVMp were found modified in conventional phosphothreonine and phosphoserine residues that are placed at precise sites in these proteins (Fig. 1 and 2). There were about 15 reproducibly resolved tryptic phosphopeptides in the VP fingerprints (Fig. 2), which is half the theoretical number of tryptic peptides of the VP-2 sequence that could be expected to harbor Ser or Thr residues (7). This observation indicates that the phosphorylated residues must be distributed along different domains of the MVMp capsid subunits.

Several data indicate that the phosphorylation sites in the VP subunits of the MVMp capsid are occupied at a low stoichiometry. For example, a high concentration of [^{32}P]phosphate in the culture media during MVMp infection was necessary to obtain sufficient amounts of labeled VP proteins, and the incorporated counts were always much lower than the ones obtained from the same sample in the NS-1 phosphoprotein (our unpublished observations). Likewise, the phosphate radicals are not resolved in the MVMp capsid structure (M. Agbandje-McKenna, personal communication) or in the MVMi strain for which an atomic structure is available (3) and in which the VP-2 pattern of phosphorylation is similar to MVMp (our unpublished observations). Even the level of substitution differed markedly among the phosphorylated positions, and so the phosphates in the many reproducible phosphopeptides giving weak signals in the 2D fingerprints (Fig. 2) must be represented at a very low rate in the MVMp capsid. However, while an effect triggered by phosphorylation on the activity of single or oligomeric proteins may require substitution in most functional or regulatory subunits, MVMp capsid functions could be modulated by phosphate radicals incorporated in a few of the 60 VP protein subunits forming the capsid. Thus, any of the identified VP phosphopeptides has potential utility for our understanding of the MVMp capsid functions.

A major result derived from this study was the finding that the two types of protein subunits occupying equivalent positions in the T=1 MVMp capsid show distinct patterns of phosphorylation. Phosphopeptides D to O resolved in the 2D fingerprints were present in the VP-1 and VP-2 proteins (Fig. 2), and thus they should map in the common sequence of both polypeptides. However, the major phosphopeptides were specific for either type of protein subunit: peptides P to S were exclusively present in VP-1, and peptides A to C were found only in VP-2. Except for phosphopeptide B, corresponding to the exposed VP-2 N-terminal domain (see below), the phosphorylation sites were inaccessible to trypsin cleavage (Fig. 3B) and must be localized in the ordered regions of the MVM capsid subunits, namely, the β-barrel and the large loops (3, 69), although some of the P to S peptides may lie in the unordered VP-1 specific region. This differential phosphorylation of the VP subunits may contribute to a metastable state of the capsid necessary for the conformational transitions observed during cell entry in other virus systems (21) or may determine some of the specific functions played by these polypeptides in the MVMp life cycle, like VP-1 controlled exposure (19) and requirement for the infectivity of the particles (63) or that of VP-2 for capsid formation and tropism (34, 63) as well as for the nuclear transport of capsid protein oligomers (33). The specificity in some of the residues acting as phosphate acceptors for each type of capsid protein subunit is

a newly recognized characteristic of icosahedral viruses that may become of wide biological interest.

The major phosphorylated domain of the MVMp particle. VP-2 is the major protein component of MVM, constituting an estimated 50 of the 60 protein subunits of the T=1 capsid. The most prominent phosphopeptide of VP-2 was peptide B; thus, this portion of VP-2 harbors the bulk of the phospho-label of the MVMp capsid and of immature virions. A comparison of ^{35}S-tryptic maps of MVMp structural polypeptides allowed us to localize peptide B to the VP-2 N-terminal domain, accounting for the important loss of ^{32}P-label detected in virions during VP-2 to VP-3 processing in vitro and in vivo. Since the label of peptide B was due exclusively to phosphoserine, viruses mutated on every serine residue of peptide B were constructed, grown, and purified. The conservation of peptide B as the major phosphopeptide in ^{32}P-labeled empty capsids of the four point mutants (Fig. 5) indicated the presence of multiple phosphoserine residues in this VP-2 domain. Mapping the positions of these residues was complicated by the masking of chymotrypsin and V8 proteases cleavage sites by neighboring phosphate radicals. Some mutations released phosphorylation, exposing the cleavage sites, which demonstrated the protection phenomenon itself and eventually allowed the assignment of positions 2, 6, and 10 as the three phosphorylated serines in the wt protein subunits (Fig. 6). Only the V8 recognition site at position D3 seemed incapable of being cleaved, given the identical electrophoretic mobility of the two V8 phosphopeptides of the S2G and S6G mutant peptides. This site may be blocked by a nearby nonphosphorylated N-terminal modification similar to the one that prevented chemical sequencing of the amino terminus of VP-2 in a highly related parvovirus (48).

The major phosphorylated domain of the MVMp capsid is placed at a region of VP-2 not resolved in the MVM or CPV crystal structures (3, 69) due to its unordered or flexible disposition on the viral surface. This domain, capable of inducing the synthesis of neutralizing antibodies (37), is cleaved in a high proportion of the VP-2 subunits of DNA-containing virions during internalization in the cells (19, 47, 55). It has been postulated that the virion channel is the site of externalization of the N terminus of VP-2 subunits at fivefold axes, enabling cleavage to form VP-3 (69). Since this cleavage does not occur in empty capsids neither in VP-1 subunits, we postulated that a charge repulsion between the three phosphoserines of peptide B in VP-2 and the encapsidated DNA could determine the specific externalization of the VP-2 N-terminal domain in full virions. This hypothesis was evaluated by using virions mutated at the serine residues grown in vivo, as well as analyzed in vitro. Virions lacking phosphopeptide B (mutant 4S/G) grown in culture carried normal proportion of VP-3 subunits (Fig. 7B), and VP-2 subunits of virions recovered early in the infection could be cleaved to VP-3 with trypsin in vitro similarly to the wt VP-2 subunits (Fig. 7C). Thus, phosphorylation is not important for externalization of the VP-2 N-terminal domain, which is consistent with the recent observation that heat can externalize this domain in empty native and virus-like particles (29), suggesting that physical steric forces, rather than the involvent of electrostatic charges, are responsible for VP-2 extrusion during viral DNA encapsidation.

Biological role of VP-2 N-terminal phosphorylation. Viruses mutated at the VP-2 N-terminal phosphorylation sites grew more slowly than the wt virus, although they could be recovered and purified in sufficient amounts for chemical analysis and phenotypic characterization. The inoculation of monolayers of permissive cells with normalized amounts of virion particles showed a number of cells expressing MVM capsid proteins comparable between the wt and the S2G and 4S/G

mutants (Fig. 8C). Therefore, the VP-2 N-terminal phosphates are not essential for the early steps of the MVMp infectious cycle, namely, receptor interaction, internalization, and nuclear targeting of the incoming particle. Moreover, the synthesis of capsid proteins occurred to normal levels, and the VP proteins translocated to the nucleus of the infected cells (Fig. 8D). The nuclear transport of many karyophilic viral structural complexes is either up- or down-regulated by phosphate radicals that generally act on their nuclear localization sequence (23, 33, 40, 73). In contrast to common linear nuclear localization sequences, the nuclear transport of synthesized VP-2 subunits required the configuration of a β-strand motif (41) which is sensitive to changes that affect the configuration of the polypeptide, such as distorting point mutations or distant deletions. The efficient nuclear targeting of the 4S/G mutant proteins suggests that the phosphorylation of the VP-2 N terminus does not contribute to the proper folding of the polypeptide chain, which is in agreement with the final unordered disposition of this domain outside the capsid shell (3, 69).

Even when involved neither in capsid protein processing nor in the initiation of the infection, an impairment of VP-2 N-terminal phosphorylation severely affected the MVMp life cycle. VP-2 phosphorylation mutants can initiate infection but do not spread efficiently to neighboring cells, since their plaque-forming capacity per immunofluorescence-positive infected cell was 10 to 20 times lower than that of the wt (Fig. 8) and the plaques were smaller. Steps likely to be affected by VP-2 N-terminal phosphorylation include processes occurring late in the MVM life cycle, such as assembly, genome encapsidation, and virus egress from the cells. In fact, this region of VP-2 seems to play multiple roles in the MVM life cycle, since virions mutated near the VP-2 cleavage region also showed a deficient plaque formation phenotype, mainly because several early infection steps were affected (71). It could even be that phosphates simply play a passive role in these processes. Indeed, the phosphate radicals efficiently protect the VP-2 N terminus against different proteases in vitro, since phosphorylation at the three serine residues 2, 6, and 10 is necessary for full protection (Fig. 6). Phosphorylation could be required in vivo to protect the true function of the VP-2 N-terminal sequence excluded from the viral capsid shell under different intracellular environments.

Among the three phosphorylated residues of the MVMp VP-2 N terminus, only serine 2 is completely conserved within the genus of the autonomous parvoviruses (16). It is worth noting that phosphorylation at this position was the most important for MVMp plaque formation, even though the other two phosphorylated positions seem to cooperate for infectivity (Fig. 8A and B). The availability of phosphorylable residues in the VP-2 N terminus may influence the interaction of parvoviruses with their hosts. Interestingly, the VP-2 capsid protein of the immunosuppressive strain of MVM (MVMi), a virus displaying different tropism and pathogenicity (13, 50, 56, 57), is also phosphorylated in Ser and Thr residues and its phosphopeptide map is undistinguishable from that of MVMp (our unpublished observations), but serine at position 6 is not conserved in this virus (7). Alternative capsid phosphorylations by Ser/Thr kinases in different cellular types may underlie the dependence of parvovirus multiplication on cellular physiology (18, 59, 62, 65) and neoplastic transformation (45, 54).

ACKNOWLEDGMENTS

REFERENCES

1. **Agbandje, M., R. McKenna, M. G. Rossmann, M. L. Strassheim, and C. R. Parrish.** 1993. Structure determination of feline panleukopenia virus empty particles. Proteins **16:**155–171.
2. **Agbandje, M., S. Kajigaya, R. McKenna, N. S. Young, and M. G. Rossmann.** 1994. The structure of human parvovirus B19 at 8 Å resolution. Virology **203:**106–115.
3. **Agbandje-McKenna, M., A. L. Llamas-Sainz, F. Wang, P. Tattersall, and M. G. Rossmann.** 1998. Functional implications of the structure of the murine parvovirus, minute virus of mice. Structure **6:**1369–1381.
4. **Anders, D. G., and R. A. Consigli.** 1983. Comparison of non-phosphorylated and phosphorylated species of polyomavirus major capsid protein VP1 and identification of the major phosphorylation region. J. Virol. **48:**206–217.
5. **Antonietti, J.-P., R. Sahli, P. Beard, and B. Hirt.** 1988. Characterization of the cell type-specific determinant in the genome of minute virus of mice. J. Virol. **62:**552–557.
6. **Aoki, H., J. Hayashi, M. Moriyama, Y. Arakawa, and O. Hino.** 1999. Hepatitis C virus core protein interacts with 14-3-3 protein and activates the kinase Raf-1. J. Virol. **74:**1736–1741.
7. **Astell, C. R., E. M. Gardiner, and P. Tattersall.** 1986. DNA sequence of the lymphotropic variant of minute virus of mice, MVM(i), and comparison with the DNA sequence of the fibrotropic prototype strain. J. Virol. **57:**656–669.
8. **Ball-Goodrich, L. J., and P. Tattersall.** 1992. Two amino acid substitutions within the capsid are coordinately required for acquisition of fibrotropism by the lymphotropic strain of minute virus of mice. J. Virol. **66:**3415–3423.
9. **Bloom, M. E., D. A. Martin, L. L. Oie, M. E. Huhtanen, F. Costello, J. B. Wolfinbarger, S. F. Hayes, and M. Agbandje-Mckenna.** 1997. Expression of Aleutian mink disease parvovirus capsid proteins in defined segments: localization of immunoreactive sites and neutralizing epitopes to specific regions. J. Virol. **71:**705–714.
10. **Boissy, R., and C. R. Astell.** 1985. An Escherichia coli recBC sbc BrecF host permits the deletion-resistant propagation of plasmid clones containing the 5′-terminal palindrome of minute virus of mice. Gene **35:**179–185.
11. **Bolen, J. B., D. G. Anders, J. Trempy, and R. A. Consigli.** 1981. Differences in the subpopulations of the structural proteins of polyoma virions and capsids: biological functions of the multiple VP-1 species. J. Virol. **37:**80–91.
12. **Boyle, W. J., P. van der Geer, and T. Hunter.** 1991. Phosphopeptide mapping and phosphoamino acid analysis by two-dimensional separation on thin-layer cellulose plates. Methods Enzymol. **201:**110–149.
13. **Brownstein, D. G., A. L. Smith, R. O. Jacoby, E. A. Johnson, G. Hansen, and P. Tattersall.** 1991. Pathogenesis of infection with a virulent allotropic variant of minute virus of mice and regulation by host genotype. Lab. Investig. **65:**357–363.
14. **Caspar, D. L., and A. Klug.** 1962. Physical principles in the construction of regular viruses. Cold Spring Harbor Symp. Quant. Biol. **27:**1–24.
15. **Chang, S.-F., J.-Y. Sgro, and C. R. Parrish.** 1992. Multiple amino acids in the capsid structure of canine parvovirus coordinately determine the canine host range and specific antigenic and hemagglutination properties. J. Virol. **66:**6858–6867.
16. **Chapman, M. S., and M. G. Rossman.** 1993. Structure, sequence, and function correlations among parvoviruses. Virology **194:**491–508.
17. **Clipman, P. R., M. Agbandje-Mckenna, S. Kajigaya, K. E. Brown, N. S. Young, T. S. Baker, and M. G. Rossmann.** 1996. Cryo-electron microscopy studies of empty capsids of human parvovirus B19 complexed with its cellular receptor. Proc. Natl. Acad. Sci. USA **93:**7502–7506.
18. **Cotmore, S. F., and P. Tattersall.** 1987. The autonomously replicating parvoviruses of vertebrates. Adv. Virus Res. **33:**91–173.
19. **Cotmore, S. F., A. M. D'Abramo, C. M. Ticknor, and P. Tattersall.** 1999. Controlled conformational transitions in the MVM virions expose the VP1 N-terminus and viral genome without particle disassembly. Virology **254:**169–181.
20. **Crawford, L. V.** 1966. A minute virus of mice. Virology **29:**605–612.
21. **Curry, S., M. Chow, and J. M. Hogle.** 1996. The poliovirus 135S particle is infectious. J. Virol. **70:**7125–7131.
22. **Fang, N. X., I. H. Frazer, J. Zhou, and G. J. Fernando.** 1999. Post translational modifications of recombinant human papillomavirus type 6b major capsid protein. Virus Res. **60:**113–121.
23. **Gallay, P., S. Swingler, J. Song, F. Bushman, and D. Trono.** 1995. HIV nuclear import is governed by the phosphotyrosine-mediated binding of matrix to the core domain of the integrase. Cell **83:**569–576.
24. **Garcea, R. L., and T. L. Benjamin.** 1983. Host range transforming gene of polyoma virus plays a role in virus assembly. Proc. Natl. Acad. Sci. USA **80:**3613–3617.
25. **Garcea, R. L., D. A. Talmage, A. Harmatz, R. Freund, and T. L. Benjamin.** 1989. Separation of host range from transformation functions of the hr-t gene of polyomavirus. Virology **168:**312–319.

26. **Garcea, R. L., K. Ballmer-Hofer, and T. L. Benjamin.** 1985. Virion assembly defect of polyomavirus hr-t mutants: underphosphorylation of major capsid protein VP-1 before viral DNA encapsidation. J. Virol. **54:**311–316.

27. **Gardiner, E. M., and P. Tattersall.** 1988. Mapping of the fibrotropic and lymphotropic host range determinants of the parvovirus minute virus of mice. J. Virol. **62:**2605–2613.

28. **Ghabrial, S. A., and W. M. Havens.** 1992. The *Helminthosporium victoriae* 190S mycovirus has two forms distinguishable by capsid protein composition and phosphorylation state. Virology **188:**657–665.

29. **Hernando, E., A. L. Llamas-Saiz, C. Foces-foces, R. McKenna, I. Portman, M. Agbandje-McKenna, and J. M. Almendral.** 2000. Biochemical and physical characterization of parvovirus minute virus of mice virus-like particles. Virology **267:**299–309.

30. **Hewat, E., N. Verdaguer, I. Fita, W. Blakemore, S. Brooks, A. King, J. Newman, E. Domingo, M. G. Mateu, and D. Stuart.** 1997. Structure of the complex of a Fab fragment of a neutralising antibody with foot-and-mouth disease virus. Positioning of a highly mobile loop. EMBO J. **16:**1492–1500.

31. **Kamps, M. P.** 1991. Determination of phosphoamino acid composition by acid hydrolysis of protein blotted to immobilon. Methods Enzymol. **201:**21–27.

32. **Kann, M., and W. H. Gerlich.** 1994. Effect of core protein phosphorylation by protein kinase C on encapsidation of RNA within core particles of hepatitis B virus. J. Virol. **68:**7993–8000.

33. **Kann, M., B. Sodeik, A. Vlachou, W. H. Gerlich, and A. Helenius.** 1999. Phosphorylation-dependent binding of hepatitis B virus core particles to the nuclear pore complex. J. Cell Biol. **145:**45–55.

34. **Kaptur, P. E., B. J. McCreedy, Jr., and D. S. Lyles.** 1992. Sites of in vivo phosphorylation of vesicular stomatitis virus matrix protein. J. Virol. **66:**5384–5392.

35. **Klug, A.** 1983. Architectural design of spherical viruses. Nature **303:**378–379.

36. **Kunkel, T. A.** 1985. Rapid and efficient site-specific mutagenesis without phenotypic selection. Proc. Natl. Acad. Sci. USA **82:**488–492.

37. **Langeveld, J. P. M., J. I. Casal, C. Vela, K. Dalsgaard, S. H. Smale, W. Puijk, and R. H. Meloen.** 1993. B-cell epitopes of canine parvovirus: distribution on the primary structure and exposure on the viral surface. J. Virol. **67:**765–772.

38. **Leader, D. P., and M. Katan.** 1988. Viral aspects of protein phosphorylation. J. Gen. Virol. **69:**1441–1464.

39. **Li, M., and R. L. Garcea.** 1994. Identification of threonine phosphorylation sites on the polymavirus major capsid protein VP-1: relationship to the activity of middle T antigen. J. Virol. **68:**320–327.

40. **Liao, W., and J.-H. Ou.** 1995. Phosphorylation and nuclear localization of the hepatitis B virus core protein: significance of serine and three repeated SPRRR motifs. J. Virol. **69:**1025–1029.

41. **Lombardo, E., J. C. Ramírez, M. Agbandje-McKenna, and J. M. Almendral.** 2000. A β-stranded motif drives capsid protein oligomers of the parvovirus minute virus of mice into the nucleus for viral assembly. J. Virol. **74:**3804–3814.

42. **Maxwell, I. H., A. L. Spitzer, F. Maxwell, and D. J. Pintel.** 1995. The capsid determinant of fibrotropism for the MVMp strain of minute virus of mice functions via VP2 and not VP1. J. Virol. **69:**5829–5832.

43. **McKenna, R., N. H. Olson, P. R. Chipman, T. S. Baker, T. F. Booth, J. Christensen, B. Aasted, J. M. Fox, M. E. Bloom, J. B. Wolfinbarger, and M. Agbandje-McKenna.** 1999. Three-dimensional structure of Aleutian mink disease parvovirus: implications for disease pathogenicity. J. Virol. **73:**6882–6891.

44. **Merchlinsky, M. J., P. J. Tattersall, J. J. Leary, S. F. Cotmore, E. M. Gardiner, and D. C. Ward.** 1983. Construction of an infectious molecular clone of the autonomous parvovirus minute virus of mice. J. Virol. **47:**227–232.

45. **Mousset, S., and J. Rommelaere.** 1982. Minute virus of mice inhibits cell transformation by simian virus 40. Nature (London) **300:**537–539.

46. **Mu, J.-J., H.-L. Wu, B.-L. Chiang, R.-P. Chang, D.-S. Chen, and P.-J. Chen.** 1999. Characterization of the phosphorylated forms and the phosphorylated residues of hepatitis virus delta antigens. J. Virol. **73:**10540–10545.

47. **Paradiso, P. R.** 1981. Infectious process of the parvovirus H-1: correlation of protein content, particle density, and viral infectivity. J. Virol. **39:**800–807.

48. **Paradiso, P. R., K. R. Williams, and R. L. Constantino.** 1984. Mapping of the amino terminus of the H-1 parvovirus major capsid protein. J. Virol. **52:**77–81.

49. **Parrish, C. R.** 1991. Mapping specific functions in the capsid structure of canine parvovirus and feline panleukopenia virus using infectious plasmid clones. Virology **183:**195–205.

50. **Ramírez, J. C., A. Fairén, and J. M. Almendral.** 1996. Parvovirus minute virus of mice strain i multiplication and pathogenesis in the newborn mouse brain is restricted to proliferative areas and to migratory cerebellar young neurons. J. Virol. **70:**8109–8116.

51. **Richards, R., P. Linser, and R. W. Armentrout.** 1977. Kinetics of assembly of a parvovirus minute virus of mice, in synchronized rat brain cells. J. Virol. **22:**778–793.

52. **Rossmann, M. G., and J. E. Johnson.** 1989. Icosahedral RNA virus structure. Annu. Rev. Biochem. **58:**533–573.

53. **Rossmann, M. G., R. McKenna, L. Tong, D. Xia, J.-B. Dai, H. Wu, H.-K. Choi, and R. E. Lynch.** 1992. Molecular replacement real-space averaging. J. Appl. Crystallogr. **25:**166–180.

54. **Salomé, N., B. van Hille, N. Duponchel, G. Meneguzzi, F. Cuzin, J. Rommelaere, and J. J. Cornelis.** 1990. Sensitization of transformed rat cells to parvovirus MVMp is restricted to specific oncogenes. Oncogenes **5:**123–130.

55. **Santarén, J. F., J. C. Ramírez, and J. M. Almendral.** 1993. Protein species of the parvovirus minute virus of mice strain MVMp: involvement of phosphorylated VP-2 subtypes in viral morphogenesis. J. Virol. **67:**5126–5138.

56. **Segovia, J. C., A. Real, J. A. Bueren, and J. M. Almendral.** 1991. *In vitro* myelosuppressive effects of the parvovirus minute virus of mice (MVMi) on hematopoietic stem and committed progenitor cells. Blood **77:**980–988.

57. **Segovia, J. C., J. M. Gallego, J. A. Bueren, and J. M. Almendral.** 1999. Severe leukopenia and dysregulated erythropoiesis in SCID mice persistently infected by the parvovirus minute virus of mice. J. Virol. **73:**1774–1784.

58. **Shang-Zhong, X., and M. Banks.** 1991. Baculovirus expression of the human papillomavirus type 16 capsid proteins: detection of L1–L2 protein complexes. J. Gen. Virol. **72:**2981–2988.

59. **Siegl, G.** 1984. Biology and pathogenicity of autonomous parvoviruses, p. 297–362. *In* K. I. Berns (ed.), The parviruses. Plenum Press, Inc., New York, N.Y.

60. **Siegl, G., R. C. Bates, K. I. Berns, B. J. Carter, D. C. Kelly, E. Kurstak, and P. Tattersall.** 1985. Characteristic and taxonomy of parvoviridae. Intervirology **23:**61–73.

61. **Simpson, A. A., P. R. Chipman, T. S. Baker, P. Tijssen, and M. G. Rossmann.** 1998. The structure of an insect parvovirus (*Galleria mellonella* densovirus) at 3.7 Å resolution. Structure **6:**1355–1367.

62. **Spalholz, B. A., and P. Tattersall.** 1983. Interaction of minute virus of mice with differentiated cells: strains-dependent target cell specificity is mediated by intracellular factors. J. Virol. **46:**937–943.

63. **Strassheim, M. L., A. Gruenberg, P. Veijalainen, J.-Y. Sgro, and C. R. Parrish.** 1994. Two dominant neutralizing antigenic determinants of canine parvovirus are found on the threefold spike of the capsid. Virology **198:**175–184.

64. **Tattersall, P.** 1978. Parvovirus protein structure and virion maturation, p. 53–72. *In* D. C. Ward and P. Tattersall (ed.), Replication of mammalian parvovirus. Cold Spring Harbor Laboratory, Cold Spring Harbor, N.Y.

65. **Tattersall, P.** 1978. Susceptibility to minute virus of mice as a function of host cell differentiation, p. 131–149. *In* D. C. Ward and P. Tattersall (ed.), Replication of mammalian parvovirus. Cold Spring Harbor Laboratory, Cold Spring Harbor, N.Y.

66. **Tattersall, P., and J. Bratton.** 1983. Reciprocal productive and restrictive virus-cell interaction of immunosuppressive and prototype strains of minute virus of mice. J. Virol. **46:**944–955.

67. **Tattersall, P., A. J. Shatkin, and D. C. Ward.** 1977. Sequence homology between the structural polypeptides of minute virus of mice. J. Mol. Biol. **111:**375–394.

68. **Tattersall, P., P. J. Cawte, A. J. Shatkin, and D. C. Ward.** 1976. Three structural polypeptides coded for by minute virus of mice, a parvovirus. J. Virol. **20:**273–289.

69. **Tsao, J., M. S. Chapman, M. Agbandje, W. Keller, K. Smith, H. Wu, M. Luo, T. J. Smith, M. G. Rossmann, R. W. Compans, and C. R. Parrish.** 1991. The three-dimensional structure of canine parvovirus and its functional implications. Science **251:**1456–1464.

70. **Tsuzuki, J., and R. B. Luftig.** 1983. The Adenovirus type 5 capsid protein IIIa is phosphorylated during an early stage of infection in HeLa cells. Virology **129:**529–533.

71. **Tullis, G. E., L. R. Burger, and D. J. Pintel.** 1992. The trypsin-sensitive RVER domain in the capsid proteins of minute virus of mice is required for efficient cell binding and viral infection but not for proteolytic processing *in vivo*. Virology **191:**846–857.

72. **Tullis, G. E., L. R. Burger, and D. J. Pintel.** 1993. The minor capsid protein VP1 of the autonomous parvovirus minute virus of mice is dispensable for encapsidation of progeny single-stranded DNA but is required for infectivity. J. Virol. **67:**131–141.

73. **Whittaker, G. I., I. Kemler, and A. Helenius.** 1995. Hyperphosphorylation of mutant influenza virus matrix protein, M1, causes its retention in the nucleus. J. Virol. **71:**1850–1856.

74. **Willwand, K., and B. Hirt.** 1993. The major capsid protein VP2 of minute virus of mice (MVM) can form particles which bind to the 3′-terminal hairpin of MVM replicative-form DNA and package single-stranded viral progeny DNA. J. Virol. **67:**5660–5663.

75. **Yu, M., and J. Summers.** 1994. Multiple functions of capsid protein phosphorylation in duck hepatitis B virus multiplication. J. Virol. **68:**4341–4348.